A Hidden Markov Model Approach to Neuron Firing Patterns

Anne-Claude Camproux,*# François Saunier,§ Guy Chouvet,§ Jean-Christophe Thalabard,¶ and Guy Thomas*
*Département de Biostatistique et Informatique Médicale, INSERM U 444, 75475 Paris Cedex 10; #Département de Biomathématiques, CHU Pitié-Salpêtrière, 75634 Paris Cedex 13; §Neuropharmacologie et Neurochimie, INSERM CJF 95-06, Université C. Bernard Lyon I, 69373 Lyon Cedex 08; and ¶CNRS URA 1454, Faculté Lyon-Sud, 69600 Oullins, France

ABSTRACT Analysis and characterization of neuronal discharge patterns are of interest to neurophysiologists and neuropharmacologists. In this paper we present a hidden Markov model approach to modeling single neuron electrical activity. Basically the model assumes that each interspike interval corresponds to one of several possible states of the neuron. Fitting the model to experimental series of interspike intervals by maximum likelihood allows estimation of the number of possible underlying neuron states, the probability density functions of interspike intervals corresponding to each state, and the transition probabilities between states. We present an application to the analysis of recordings of a locus coeruleus neuron under three pharmacological conditions. The model distinguishes two states during halothane anesthesia and during recovery from halothane anesthesia, and four states after administration of clonidine. The transition probabilities yield additional insights into the mechanisms of neuron firing.

INTRODUCTION

Central catecholaminergic neurons, such as midbrain dopaminergic (DA) neurons of the substantia nigra and the ventral tegmental area, and noradrenergic neurons of the locus coeruleus, which are involved in motor functions and attentional mechanisms, and in behavioral adaptation to the environment, respectively, have been observed to fire in two primary patterns: a "pacemaker" pattern and a "bursty" pattern (Grace and Bunney, 1984; Gonon, 1988; Saunier et al., 1993). A pattern is defined as the interval dispersion and sequence, disregarding the average rate of firing (Bullock and Horridge, 1965; Segundo et al., 1995). "Pacemaker" patterns correspond to a single type of interval, i.e., a "pacemaker neuron" fires spikes at intervals all practically equal to their average. "Bursty" patterns correspond to two clearly separate categories of intervals in which several short intervals alternate with a few single long ones.

Activation of central catecholaminergic neurons by sensory stimuli or pharmacological agents may alter their discharge patterns. Moreover, electrical stimulation delivered in bursts has been shown to be more effective than regularly spaced discharges in increasing metabolic activity and catecholamine release, independently of the mean discharge rate (Gonon, 1988). Typically, drug effects have been analyzed in terms of 1) increases or decreases in mean discharge rates, and, to take into account changes in discharge pattern, 2) the degree to which these neurons exhibit bursting activity (Carlson and Foote, 1992).

Whereas in many instances the occurrence of bursts in single-neuron recordings is readily recognized by eye, quantitative analysis and comparison of discharge patterns clearly required some more formal definition. Using 75 recordings of DA neurons considered to have bursting activity, Grace and Bunney (1984) proposed empirical criteria for defining bursting activity. They defined the onset of a burst as an interspike interval shorter than 80 ms and the termination of a burst by the next interspike interval longer than 160 ms. The limitation of this approach is that the definition of a burst lacks flexibility: the criteria were initially used to quantify bursting activity of neurons exhibiting a mean firing rate of 4–5 Hz and proved inadequate for cells firing at higher rates (Chergui et al., 1993). More generally, burst analysis amounts to a binary description of patterns, spikes, or the interspike intervals separating them, either within or outside bursts; this may thus lead to inefficient recognition of discharge pattern changes in some contexts.

Several attempts have been proposed to circumvent these limitations. Some authors combined the analysis of bursting activity as defined by Grace and Bunney (1984) with population characteristics of interspike intervals (Charléty et al., 1991; Chergui et al., 1993; Saunier et al., 1993). Shepard and German (1988) proposed definitions for three firing patterns, called regular, irregular, or bursting. Finally, Carlson and Foote (1992) used time-series measures such as return maps and phase portraits to examine patterns in terms of the ordering of interspike intervals.

In this paper we present a stochastic model approach to the problem of characterizing different firing patterns and describing the heterogeneity of interspike intervals in single-cell recordings. This is achieved within the context of hidden Markov models (HMM), the aim of which is to reconstruct a "hidden" sequence of states of a system from an observable output whose probability law depends on the underlying state. This approach was used recently by

Received for publication 26 February 1996 and in final form 27 August 1996.

Address reprint requests to Dr. Anne-Claude Camproux, Département de Biomathématiques, 91, bd de l'Hôpital, CHU Pitié Salpêtrière, 75634 Paris Cedex 13. Tel.: 33-1-40-77-96-14; Fax: 33-1-45-86-56-85; E-mail: acc@biomath.jussieu.fr.

0006-3495/96/11/2404/09 $2.00

Seidemann et al. (1996) to analyze recordings of single cells in the frontal cortex of monkeys. Other fields of applications are speech recognition (Baum et al., 1970), cardiac arrhythmias (Coast et al., 1990), seizures in epileptic patients (Albert, 1991), modeling of anion channels (Morier and Sauvé, 1994) and proteins (Krogh et al., 1994), and animal behavior (Macdonald and Raubenheimer, 1995).

THEORY AND METHODS

To justify our approach let us first consider the three artificial firing patterns illustrated in Fig. 1. Pattern *a* appears homogeneous and regular, with almost invariant intervals; it obviously qualifies as a "pacemaker." Likewise, pattern *c* would qualify as "bursty" to a naked eye evaluation. Categorization of pattern *b* is less clear and might vary among different observers. We wish to build a model aimed at discriminating and characterizing precisely such different firing modes.

Structure of the model

The basic data are the sequence $t_1, t_2, \ldots$ of successive times of occurrence of spikes. Equivalently, we work with the sequence $y_1 = t_2 - t_1, y_2 = t_3 - t_2, \ldots$ of interspike intervals.

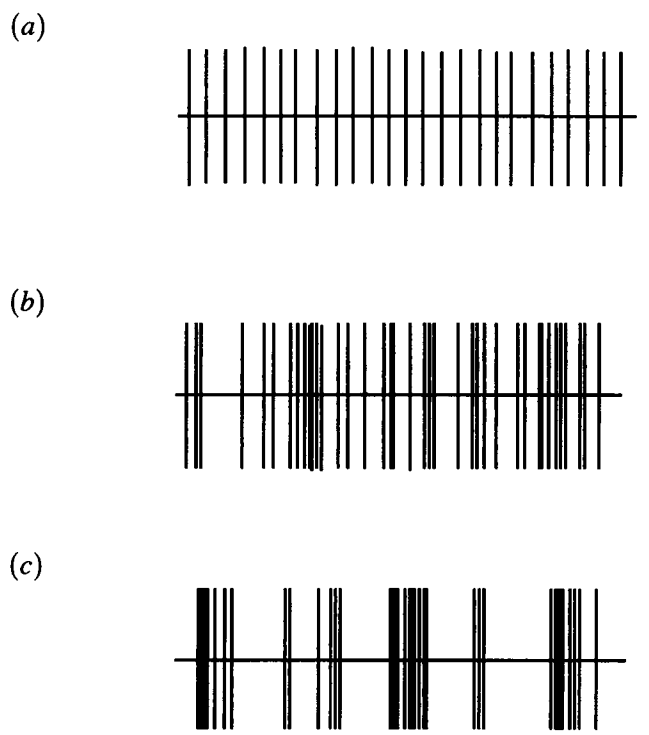

FIGURE 1 Simulated examples of neuronal discharge patterns. The horizontal axis is time, and each vertical line corresponds to a spike. By naked eye evaluation, pattern *a* would be classified as "pacemaker" and pattern *c* as "bursty." The classification of pattern *c* is less clear.

Suppose we knew that a given discharge pattern was made up of intervals of R different types. We would then assume that there are R different states of the neuron, each state corresponding to a specific type of firing mode. From this point of view, each pattern is characterized by an R value whose estimation is described below; patterns *a*, *b*, and *c* in Fig. 1 would correspond to $R = 1$, $R \geq 2$, and $R \geq 2$, respectively. The point, however, is that the states of the neuron are not observed experimentally and must be inferred from the interspike intervals they generate.

Because of unpredictable variability in the data, we cast our model in stochastic form. The observed sequence $y_1, y_2, \ldots$ of intervals is considered as a realization of a stationary sequence $Y_1, Y_2, \ldots$ of positive continuous random variables, and the corresponding sequence $i_1, i_2, \ldots$ of neuron states is considered to be a realization of a sequence $X_1, X_2, \ldots$ of discrete random variables with state space $\{1, \ldots R\}$. The possible stochastic dependence between adjacent interspike intervals is modeled as arising from dependence within the underlying neuron states. In more mathematical terms, we assume the following:

1. The random sequence $X_1, X_2, \ldots$ is a homogeneous Markov chain of order k; for the sake of clarity, and without loss of generality, we hereafter suppose $k = 1$.

2. For $j \geq 1$, the random variables $Y_1, \ldots, Y_j$ are independent conditionally on $X_1, \ldots, X_j$; moreover, for $1 \leq l \leq j$, the conditional probability density function of Y_l given $X_1, \ldots, X_j$ depends on X_l only.

Under the above assumptions, the joint stochastic behavior of the random sequences $X_1, X_2, \ldots$ and $Y_1, Y_2, \ldots$ is fully defined by specifying

- a starting distribution $\nu = (\nu_i)_{1 \leq i \leq R}$, where $\nu_i = P(X_1 = i)$
- a transition matrix $\pi = (\pi_{ii'})_{1 \leq i,i' \leq R}$, where $\pi_{ii'} = P(X_j = i' | X_{j-1} = 1)$
- for each $i = 1, \ldots, R$, the conditional density $f_i(y)$ of interspike intervals generated while the neuron is in state i.

The two-parameter Weibull family, $W_{\alpha,\beta}(t) = \alpha\beta t^{\beta-1} e^{-\alpha t^\beta}$, $\alpha, \beta > 0$, strikes a balance between flexibility and numerical tractability. However, to allow for more generality, we model the f_i's as mixtures of Weibull densities,

$$f_i(y) = \sum_{s=1}^{l_i} \gamma_{i_s} W_{\alpha_{i_s},\beta_{i_s}}(y),$$

where l_i is an integer, $\gamma_{i_s} \geq 0$ and $\Sigma_{s=1}^{l_i} \gamma_{i_s} = 1$.

For later convenience, we define $\theta_i = (\alpha_{i_1}, \beta_{i_1}, \gamma_{i_1}, \ldots, \alpha_{i_{l_i}}, \beta_{i_{l_i}}, \gamma_{i_{l_i}})$ and $\theta = (\theta_1, \ldots, \theta_R)$.

Point estimation of model parameters

Our ultimate goal, given the observation of n intervals $y_1, \ldots, y_n$, is to reconstruct the unobserved (hidden) sequence $i_1, \ldots, i_n$ of corresponding states of the neuron. The obvious approach is to determine the number R of states and then to find the most probable path $\hat{i}_1, \ldots, \hat{i}_n$ among all

possible paths in $\{1, \ldots, R\}^n$, given the observed sequence $y_1, \ldots, y_n$. To fulfill this program we proceed in successive steps to compute the conditional probabilities of the paths.

Step 1

Suppose R, k, and l_i, $i = 1, \ldots, R$, are fixed. Then the unknown parameters of the model are the starting distribution ν, the transition matrix π, and θ. It can be shown (see Appendix) that the likelihood of the model with respect to the observations $y_1, \ldots, y_n$ is

$$\sum_{1 \le i_1, \ldots, i_n \le R} \nu_{i_1} f_{i_1}(y_1) \prod_{j=1}^{n-1} \pi_{i_j i_{j+1}} f_{i_{j+1}}(y_{j+1}).$$

Unknown parameters are estimated by maximizing this expression. Computation of the likelihood function is done recursively by exploiting the underlying Markov structure of the model, following the algorithm of Baum et al. (1970), as implemented in the Forward-Backward Procedure of Rabiner (1989). Details are given in the Appendix.

Under general regularity conditions, the maximum likelihood estimators of ν, π, and θ are asymptotically Gaussian, and their asymptotic covariance matrix can be estimated as minus the inverse of the matrix of second derivatives of the log likelihood function (Lindgren, 1978).

Step 2

To determine R, k, and l_i, $i = 1, \ldots, R$, we start with the simplest model, i.e., $R = 1$, $k = 1$, $l_1 = 1$, and consider models in ascending order of complexity, by increasing R and/or k and/or l_i, $i = 1, \ldots, R$, while this results in significant improvement of the model.

Comparison of nested models is performed by the likelihood ratio test, and comparison of non-nested models is

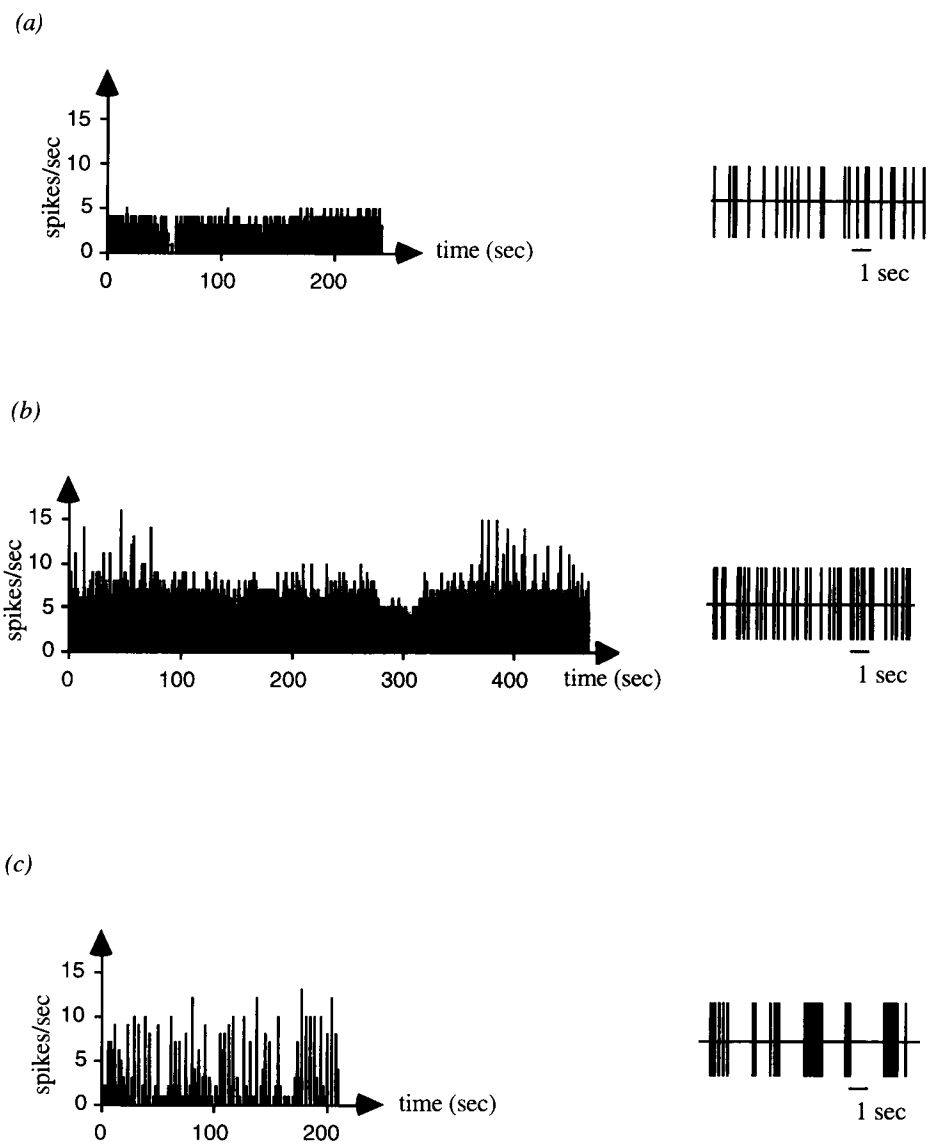

FIGURE 2 Integrated rate histograms and corresponding discharge patterns obtained from a single locus coeruleus neuron from a Sprague-Dawley rat under three different pharmacological conditions: during anesthesia with 1% halothane (recording *a*), the neuron exhibits a somewhat regular firing pattern; 20 min after recovery from halothane anesthesia (recording *b*), the firing pattern is faster and less regular; and after intravenous administration of the α_2-agonist clonidine hydrochloride (8 μg kg^{-1}) (recording *c*), resulting in a distinctly irregular phasic pattern, there is a low average firing rate and high coefficient of variation.

based on Akaike's information criterion (AIC) (Akaike, 1974).

Step 3

Once a model has been selected and its parameters have been estimated, let $\hat{P}(X_1 = i_1, \ldots, X_n = i_n | Y_1 = y_1, \ldots, Y_n = y_n)$ denote the estimated conditional probability of the path $(i_1, \ldots, i_n)$ given $y_1, \ldots, y_n$. The most probable path is found as the n-tuple $(\hat{i}_1, \ldots, \hat{i}_n)$ maximizing this probability with respect to all n-tuples $i_1, \ldots, i_n \in \{1, \ldots, R\}^n$. The maximization is done recursively using the Viterbi algorithm (Rabiner, 1989; see Appendix).

Interval estimation of model parameters

Because of the complexity of the algorithms involved in the point estimation process (see above), interval estimates of model parameters cannot be derived by analytical methods. Therefore we estimate confidence intervals using Monte Carlo simulations based on 1000 simulations of the model.

ANALYSIS OF EXPERIMENTAL DATA

In this section we apply the hidden Markov model approach to the analysis of data from a 225–250-g Sprague-Dawley rat in which the electrical activity of a single locus coeruleus neuron was recorded using stereotaxic techniques, under three pharmacological conditions: during anesthesia with 1% halothane (recording *a*), during recovery from halothane anesthesia (recording *b*), and after intravenous administration of the α_2-agonist clonidine hydrochloride (8 μg kg^{-1}) (recording *c*). Full experimental details are given in Saunier et al. (1993).

Integrated rate histograms of neuron discharges are shown in Fig. 2 together with the corresponding discharge patterns. We use the term "integrated rate histogram" for a display of the number of spikes in 1-s bins along ongoing time. The corresponding interspike interval means and coefficients of variation are presented in Table 1. Under halothane anesthesia (*a*), the neuron exhibits a somewhat regular, pacemaker firing pattern. Twenty minutes after halothane withdrawal (*b*), the firing pattern is faster and less regular. Administration of clonidine (*c*) results in a distinctly irregular bursty pattern, with a low average firing rate and high coefficient of variation.

Table 2 presents the results of the hidden Markov model analysis. For each state of the neuron, as identified by the HMM, the table shows point estimates and 95% confidence intervals of the mean, coefficient of variation, and proportion of interspike intervals generated from that state. Maximization of the likelihood function was performed with routines from IMSL (IMSL, 1987). In all instances the underlying Markov chain was found to be first-order ($k = 1$). Our procedure distinguished two states of the neuron in recordings *a* and *b*, and four states in recording *c*. Estimates of the probability density functions of the interspike intervals are plotted in Fig. 3; these estimates correspond to single Weibull densities for all states of cases *a* and *c*, and to mixtures of two Weibull densities for the two states of case *b*.

Table 3 presents point estimates and 95% confidence intervals for the means and proportions of within-burst intervals according to the criteria of Grace and Bunney (1984), in recordings *a*, *b*, and *c*. In the case of recording *a*, neither of the two states of the HMM appears to correspond to the 7% short interspike intervals within bursts according to Grace and Bunney (1984). For recording *c*, the correspondence between the population of interspike intervals generated from state 1 of the HMM and the population of the within-burst intervals of Grace and Bunney (1984) appears excellent. As for recording *b*, the correspondence looks more debatable. Fig. 4 contrasts further the results of the two approaches for recordings *b* and *c*, respectively.

TABLE 1 Mean and coefficient of variation of interspike intervals in three recordings of a single locus coeruleus neuron in a Sprague-Dawley rat

Recording	Mean (ms)	Coefficient of variation (%)
a	278.3	52
b	153.2	68
c	428.6	178

a, During halothane anesthesia; *b*, during recovery from halothane anesthesia; *c*, after administration of clonidine.

TABLE 2 Hidden Markov model analysis of discharge patterns of a single locus coeruleus neuron in a Sprague-Dawley rat

		Interspike intervals		
Recording	State	Mean (ms)	Coefficient of variation (%)	Proportion (%)
a	1	192.9	48	52
		[175.5, 215.3]	[44, 52]	[42, 62]
	2	386.7	35	48
		[355.9, 420.1]	[30, 40]	[38, 58]
b	1	91.8	38	48
		[88.9, 95.0]	[34, 42]	[39, 58]
	2	198.4	56	52
		[188.3, 211.0]	[53, 59]	[42, 61]
c	1	60.5	41	57
		[57.3, 63.9]	[37, 45]	[47, 64]
	2	179.6	65	14
		[136.8, 236.4]	[47, 79]	[7, 18]
	3	599.6	77	21
		[504.2, 719.1]	[64, 89]	[15, 32]
	4	2626.1	20	8
		[2436.4,2790.3]	[15, 25]	[6, 10]

a, During halothane anesthesia; *b*, during recovery from halothane anesthesia; *c*, after administration of clonidine. For each state of the neuron, as identified by the HMM, the table shows point estimates and 95% confidence intervals of the mean, coefficients of variation, and proportion of interspike intervals generated from that state.

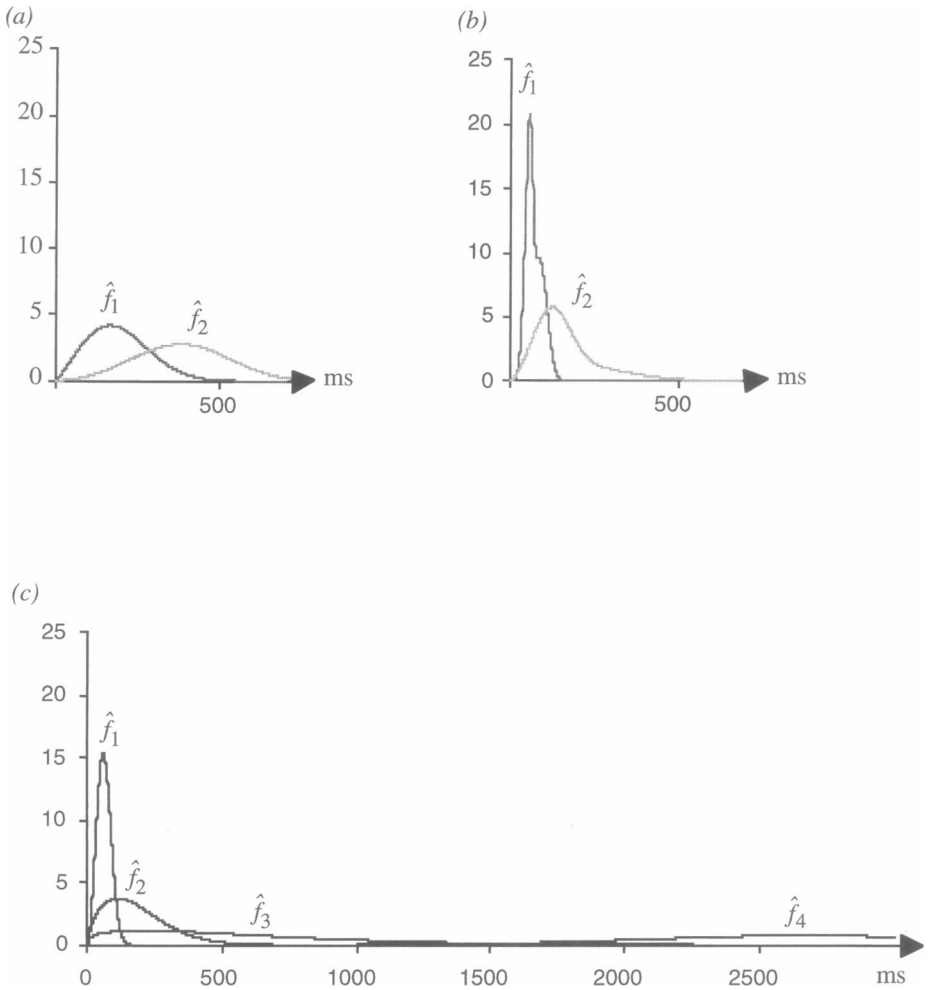

FIGURE 3 Estimated probability density functions of interspike intervals corresponding to different states of a locus coeruleus neuron. The number of states i was estimated as two during halothane anesthesia (a) and during halothane anesthesia recovery (b), and as four states in recording c after administration of clonidine. $\hat{f}_i$ denotes the estimated probability density function of interspike intervals generated from each state i.

Relationships between pairs of consecutive interspike intervals can be grasped through the visual inspection of return maps (Carlson and Foote, 1992), as illustrated in Fig. 5. Such maps can be used for the more quantitative evaluation of probabilities of occurrence of a given type of interval, given the type of the previous interval (Segundo et al., 1966). However, transition probabilities between states are directly estimated by the HMM approach, as illustrated in Fig. 6. In case a, these estimates show frequent switching between the two states, a finding reminiscent of the oscillatory phenomenon that has been observed under halothane anesthesia (Carlson and Foote, 1992). The probabilities estimated from recording b correspond to rather infrequent transitions, in agreement with the existence of bursts separated by sequences of longer intervals. Results from experiment c are probably the most interesting. Roughly, bursts of spikes (state 1) are followed by a single very long interval generated from state 4. This fact may be related to the refractory period that has been reported after repeated discharge in bursts (Bullock and Horridge, 1965; Aghajanian et al., 1977; Hoffman et al., 1995). Indeed, the interval density in state 4 is negligible for intervals of less than 1800 ms (see Fig. 3). The neuron may then switch back directly to bursting activity, or proceed through states 3 and 2, a pattern corresponding to a progressive shortening of the intervals.

TABLE 3 Burst analysis of discharge patterns of a single locus coeruleus neuron in a Sprague-Dawley rat according to the criteria of Grace and Bunney (1984)

	Interspike intervals within bursts	
Recording	Mean (ms)	Proportion (%)
a	66.9 [54.5, 70.8]	7 [5, 8]
b	80.8 [79.0, 83.4]	40 [35, 46]
c	59.5 [56.9, 62.9]	57 [49, 65]

a, During halothane anesthesia; *b*, during recovery from halothane anesthesia; *c*, after administration of clonidine. The table shows estimates and 95% confidence intervals of the mean and proportion of interspike intervals within bursts.

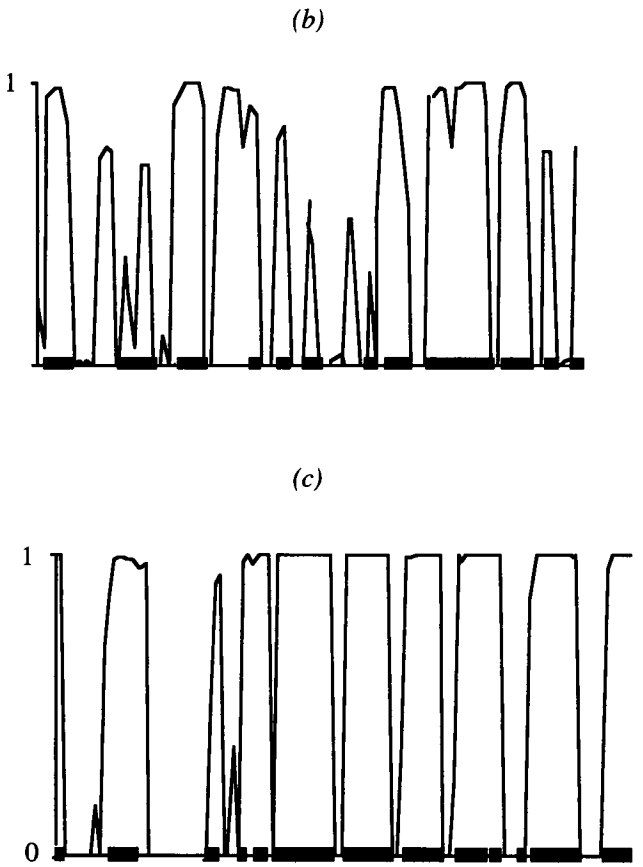

FIGURE 4 Probability that the neuron is in state 1 of the HMM, conditional on the observed sequence of interspike intervals, for 100 consecutive intervals from recordings *b* and *c*, respectively. Closed squares on the horizontal axis indicate bursting intervals according to the criteria of Grace and Bunney (1984).

DISCUSSION

We have presented a hidden Markov model aimed at characterizing neuron firing patterns and analyzing the heterogeneity of interspike intervals.

A characteristic feature of locus coeruleus neuron activity is a burst of activation in response to sensory or noxious stimulation, followed by a prolonged period of inhibition (Aghajanian et al., 1977). Neuropharmacological experiments revealed that the nucleus paragiganto-cellularis provides a potent excitatory amino acid input to the locus coeruleus, acting primarily at non-NMDA (*N*-methyl-D-aspartate) receptors, and that this pathway mediates certain sensory excitatory responses of locus coeruleus neurons (Aston-Jones et al., 1991). Furthermore, Ennis and Aston-Jones (1986) have reported that a calcium-dependent potassium conductance and a collateral noradrenergic inhibition (via α_2-adrenergic autoreceptors) were about equal in their contributions to the postactivation inhibition.

Dopaminergic neurons studied by Grace and Bunney (1984) are required for normal behavior and movements. In vivo they fire action potentials in bursts, but in vitro they discharge regularly spaced action potentials. It has been demonstrated that this burst firing is mediated via NMDA receptors (Chergui et al., 1993) and is controlled, in part, by excitatory amino acid afferents originating in the subthalamic nucleus (Chergui et al., 1994). The hyperpolarization between bursts of action potentials results from an electrogenic extrusion of sodium ions by a ouabain-sensitive pump (Johnson et al., 1992).

Thus it is tempting to speculate that state 1 as detected by HMM analysis of recordings under halothane withdrawal and after repeated injection of clonidine might correspond to such excitatory amino acid afferent inputs. Indeed, it has been shown that locus coeruleus bursting activity defined by Grace and Bunney (1984), observed after halothane withdrawal and clonidine administration, was suppressed by local application of the excitatory amino acid antagonist kynurenate (Saunier et al., 1993).

However, locus coeruleus neurons receive other excitatory and inhibitory inputs from many interconnected sources mediated by both chemical neurotransmitters and electronic coupling. In particular, the nucleus prepositus hypoglossi potently inhibits locus coeruleus neurons via a GABAergic projection acting at $GABA_A$ receptors, and serotonin selectively attenuates excitations of locus coeruleus neurons evoked by excitatory amino acids through $5\text{-}HT_{1A}$ receptors (Aston-Jones et al., 1991).

Consequently, other states detected from the HMM may represent the collective interactions of various inputs at the somato-dendritic level combined with intrinsic membrane properties. In particular, state 4, detected after clonidine administration and corresponding to the very long interspike intervals, may relate to the well-known inhibitory properties of this α_2-adrenergic agonist via somatodendritic autoreceptors (Svensson et al., 1975).

States 1 and 2 detected from the HMM under halothane anesthesia and states 2 and 3 after repeated injections of clonidine might represent a substantial oscillatory tendency in the magnitudes of consecutive interspike intervals in locus coeruleus neurons, as already observed for dopaminergic neurons (Carlson and Foote, 1992). Furthermore, state 1 under halothane anesthesia, state 2 under halothane withdrawal, and state 2 after repeated injections of clonidine might be interpreted as corresponding to the neuron's spontaneous activity.

As compared to the method of interspike interval analysis of Grace and Bunney (1984), which separates interspike intervals into within-burst or between-burst intervals, our approach, although more computationally demanding, allows a more flexible description of interspike interval heterogeneity. Other methods based on the analysis of the joint interval distribution are more detailed in essence, but the HMM approach yields direct estimation of transition probabilities between states, thus allowing deeper quantitative insight into the mechanisms underlying the observed neuron discharge patterns.

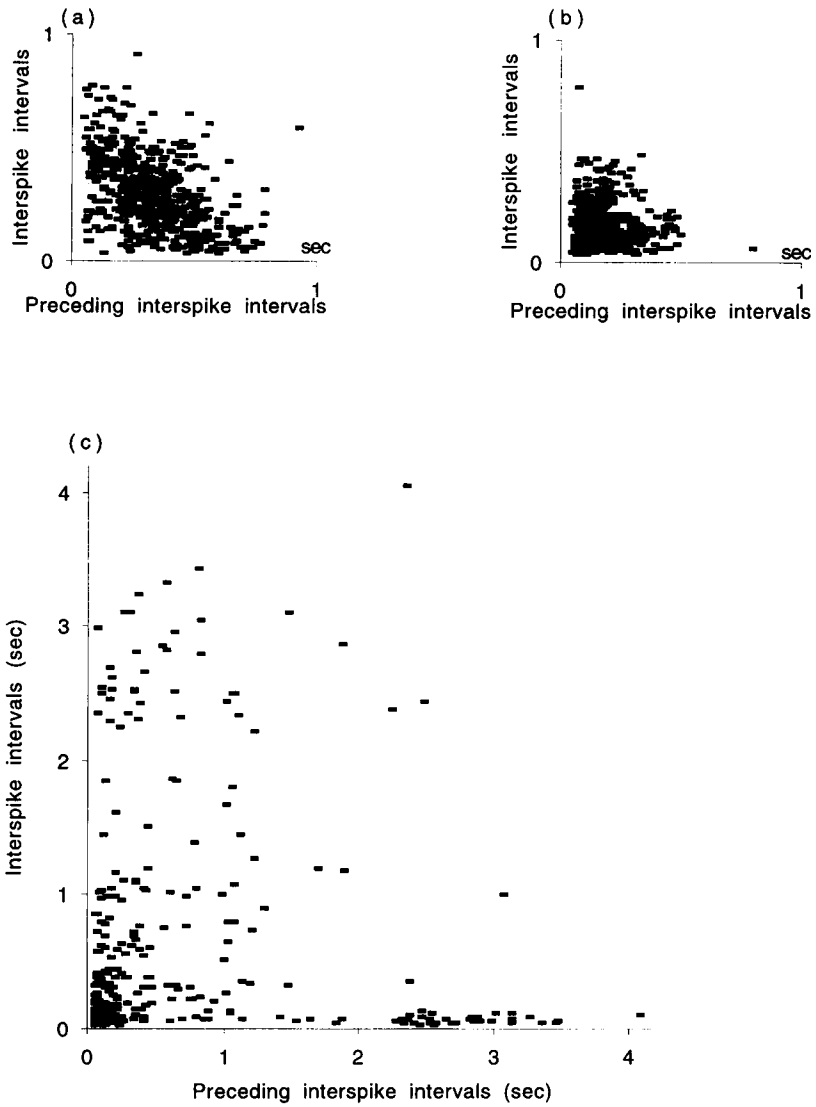

FIGURE 5 Return maps of the neuron discharge patterns under three pharmacological conditions: (*a*) during halothane anesthesia, (*b*) during recovery from halothane anesthesia, and (*c*) after administration of clonidine. The duration of each interspike interval is plotted as a function of the duration of the immediately preceding interval. The points lying about the abscissa and ordinate represent "long–short" and "short–long" pairs of interspike intervals, respectively.

APPENDIX

Likelihood computation

The likelihood $l(\theta, \nu, \pi)$ of the data $y_1, \ldots, y_n$ is defined as the joint density of the random variables $Y_1, \ldots, Y_n$ at $Y_1 = y_1, \ldots, Y_n = y_n$. To compute $l(\theta, \nu, \pi)$, we note that the joint density of $X_1, Y_1, \ldots, X_n, Y_n$ at $X_1 = i_1, Y_1 = y_1, \ldots, X_n = i_n, Y_n = y_n$ is easily written as

$$\nu_{i_1} f_{i_1}(y_1) \prod_{j=1}^{n-1} \pi_{i_j i_{j+1}} f_{i_{j+1}}(y_{j+1}),$$

so that the density of $Y_1, \ldots, Y_n$ can be obtained by summing out on all possible sequences $i_1, \ldots, i_n$ of states in $\{1, \ldots, R\}^n$:

$$l(\theta, \nu, \pi) = \sum_{1 \le i_1, \ldots, i_n \le R} \nu_{i_1} f_{i_1}(y_1) \prod_{j=1}^{n-1} \pi_{i_j i_{j+1}} f_{i_{j+1}}(y_{j+1}).$$

In this form the amount of computation is on the order of $2nR^n$ calculations; there are R^n possible state sequences, and for each such state sequence about $2n$ calculations are required for the likelihood. However, Baum et al. (1970) show how the underlying Markov structure of the model can be used to derive a recursive algorithm that only requires on the order of nR^2 calculations. We give a brief description of this algorithm, following the presentation of Rabiner (1989).

First, by the theorem of total probability, we have

$$l(\theta, \nu, \pi) = \sum_{i=1}^{R} f(y_1, \ldots, y_n \mid X_n = i) P(X_n = i),$$

where $f(y_1, \ldots, y_n | X_n = i)$ is the density of $Y_1, \ldots, Y_n$, conditional on $X_n = i$. Now the right-hand side of the above identity can be computed recursively, using the recursion formula

$$f(y_1, \ldots, y_{j+1} \mid X_{j+1} = i') P(X_{j+1} = i')$$

$$= \sum_{i=1}^{R} [f(y_1, \ldots, y_j \mid X_j = i) P(X_j = i) \pi_{ii'}] f_{i'}(y_{j+1}),$$

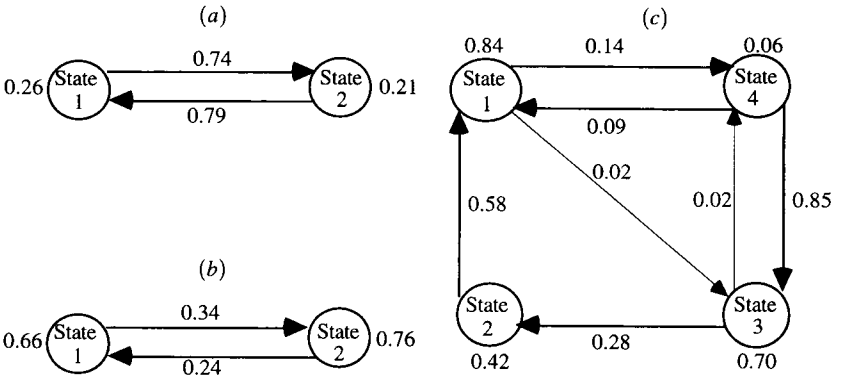

FIGURE 6 Estimates of transition probabilities between the different states of the neuron. (*a*) During halothane anesthesia, (*b*) during recovery from halothane anesthesia, (*c*) after administration of clonidine.

and the starting value

$$f(y_1 | X_1 = i)P(X_1 = i) = \nu_i f_i(y_1), \quad i = 1, \ldots, R.$$

Sequence reconstruction

Having observed a sequence of n interspike intervals $y_1, \ldots, y_n$, we try to guess the corresponding sequence of the n states of the neuron that generated these intervals. We choose to reconstruct this sequence as the n-tuple $\hat{i}_1, \ldots, \hat{i}_n$ that has the highest probability, given $y_1, \ldots, y_n$. To find this maximizing sequence, we use the Viterbi recursive algorithm (Rabiner, 1989).

First, for $1 \leq i \leq R$, let

$$\delta_1(i) = \nu(i) f_i(y_1),$$

and

$$\delta_j(i) = \max_{i_1, i_2, \ldots, i_{j-1}} P(X_1 = i_1, \ldots, X_j = i, Y_1 = y_1, \ldots, Y_j = y_j),$$

$$2 \leq j \leq n.$$

We note that $\delta_n(i)$ can be computed recursively using the identity

$$\delta_{j+1}(i') = \left[\max_{i=1,\ldots,R} \delta_j(i) \pi_{ii'} \right] f_{i'}(y_{j+1}).$$

Then we find the sequence $\hat{i}_1, \ldots, \hat{i}_n$ by descending induction, starting from

$$i_n = \underset{1 \leq i \leq R}{\operatorname{argmax}} [\delta_n(i)],$$

and using the identity

$$i_j = \underset{1 \leq i \leq R}{\operatorname{argmax}} [\delta_j(i) \pi_{i \hat{i}_{j+1}}], \quad j = n-1, n-2, \ldots, 1.$$

REFERENCES

Aghajanian, G. K., J. M. Cedarbaun, and R. Y. Wang. 1977. Evidence for norepinephrine mediated collateral inhibition of locus coeruleus neurons. *Brain Res.* 136:570–577.

Akaike, H. 1974. A new look at the statistical model identification. *IEEE Trans. Control.* 19:716–723.

Albert, P. S. 1991. A two-state Markov mixture model for a time series of epileptic seizure counts. *Biometrics.* 47:1371–1381.

Aston-Jones, G., M. T. Shipley, G. Chouvet, M. Ennis, E. Van Bockstaele, V. Pieribone, R. Shiekhattar, H. Akaoka, G. Drolet, B. Astier, P. J Charléty, R. J. Valentino, and J. T. Williams. 1991. Afferent regulation of locus coeruleus neurons: anatomy, physiology and pharmacology. *Prog. Brain Res.* 88:44–75.

Baum, L. E., T. Petrie, G. Soules, and N. Weiss. 1970. A maximization technique occurring in the statistical analysis of probabilistic functions of Markov chains. *Ann. Math. Statist.* 41:164–171.

Bullock, T. H., and G. A. Horridge. 1965. Structure and Function in the Nervous Systems of Invertebrates. W. H. Freeman and Co., San Francisco and London.

Carlson, J. H., and S. L. Foote. 1992. Oscillation of interspike interval length in substantia nigra dopamine neurons: effects of nicotine and the dopaminergic D_2 agonist LY 163502 on electrophysiological activity. *Synapse.* 11:229–248.

Charléty, P. J., J. Grenhoff, K. Cherguy, B. De la Chapelle, M. Buda, T. H. Svensson, and G. Chouvet. 1991. Burst firing of mesencephalic dopamine neurons is inhibited by somatodendritic application of kynurenate. *Acta. Physiol. Scand.* 142:105–112.

Chergui, K., H. Akaoka, C. F. Saunier, P. J. Charléty and G. Chouvet. 1994. Subthalamic nucleus modulates burst firing of rat substantia nigra dopamine neurons via NMDA receptors. *Neuroreport.* 5:1185–1188.

Chergui, K., P. J. Charléty, H. Akaoka, C. F. Saunier, J. L. Brunet, M. Buda, T. H. Svensson, and G. Chouvet. 1993. Tonic activation of NMDA receptors causes spontaneous burst discharge of rat midbrain dopamine neurons in vivo. *Eur. J. Neurosci.* 5:137–144.

Coast, D. A., G. G. Cano, and S. A. Briller. 1990. Use of hidden Markov models for electrocardiographic signal analysis. *J. Electrocardiol.* 23: 184–191.

Ennis, M., and G. Aston-Jones. 1986. Evidence for self- and neighbour-mediated post activation inhibition of locus coeruleus neurons. *Brain Res.* 374:299–305.

Gonon, F. G. 1988. Non linear relationship between impulse flow and dopamine released by rat midbrain dopaminergic neurons as studied by in vivo electrochemistry. *Neuroscience.* 24:19–28.

Grace, A. A., and B. S. Bunney. 1984. The control of firing pattern in nigral dopamine neurons: burst firing. *J. Neurosci.* 4:2877–2890.

Hoffman, R. E., S. Wei-Xing, and B. S. Bunney. 1995. Nonlinear sequence-dependent structure of nigral dopamine neuron interspike interval firing patterns. *Biophys. J.* 69:128–137.

International Mathematical and Statistical Libraries. 1987. User's Manual: Math/Library. Fortran Subroutines for Mathematical Applications, Version 1.0, softcover Ed. IMSL, Houston, TX.

Johnson, S. W., V. Seutin, and A. R. North. 1992. Burst firing in dopamine neurons induced by NMDA: role of electrogenic sodium pump. *Science.* 258:665–667.

Krogh, A., M. Brown, I. S. Mian, K. Sjölander, and D. Haussler. 1994. Hidden Markov models in computational biology. Applications to protein modeling. *J. Mol. Biol.* 235:1501–1531.

Lindgren, G. 1978. Markov regime models for mixed distributions and switching regressions. *Scand. J. Statist.* 5:81–91.

Macdonald, I. L., and D. Raubenheimer. 1995. Hidden Markov models and animal behaviour. *Biomed. J.* 6:701–712.

Morier, N., and R. Sauvé. 1994. Analysis of a novel double-barreled anion channel from rat liver rough endoplasmic reticulum. *Biophys. J.* 67: 590–602.

Rabiner, L. R. 1989. A tutorial on hidden Markov models and selected applications in speech recognition. *Proc. IEEE.* 77:275–285.

Saunier, C. F., H. Akaoka, B. De la Chapelle, P. J. Charléty, K. Cherguy, G. Chouvet, M. Buda, and L. Quintin. 1993. Activation of brain noradrenergic neurons during recovery from halothane anesthesia. *Anesthesiology.* 79:1072–1082.

Segundo, J. P., D. H. Perkel, and G. P. Moore. 1966. Spike probability in neurones: influence of temporal structure in the trains of synaptic events. *Kybernetik.* 3:67–82.

Segundo, J. P., J. F. Vibert, M. Stiber, and S. Hanneton. 1995. Periodically modulated inhibition and its post-synaptic consequences. I. General features. Influence of pre-synaptic frequency and period. *Neuroscience.* 68:657–692.

Seidemann, E., I. Meilijson, M. Abeles, H. Bergman, and E. Vaadia. 1996. Simultaneously recorded single units in the frontal cortex go through sequences of discrete and stable states in monkeys performing a delayed localization task. *J. Neurosci.* 16:752–768.

Shepard, P. D., and D. C. German. 1988. Electrophysiological and pharmacological evidence for the existence of distinct subpopulations of nigrostriatal dopaminergic neuron in the rat. *Neuroscience.* 27:537–546.

Svensson, T. H., B. S. Bunney, and G. K. Aghajanian. 1975. Inhibition of both noradrenergic and serotoninergic neurons in the brain by the alpha-adrenergic agonist clonidine. *Brain Res.* 92:291–306.